AMERICAN SOCIETY FOR MICROBIOLOGY | Applied and Environmental Microbiology

Host-Microbial Interactions | Full-Length Text

Transient infection of *Euprymna scolopes* with an engineered D-alanine auxotroph of *Vibrio fischeri*

Macey Coppinger,[1,2] Liu Yang,[3] David L. Popham,[4] Edward Ruby,[3] Eric V. Stabb[2]

AUTHOR AFFILIATIONS See affiliation list on p. 13.

ABSTRACT The symbiosis between *Vibrio fischeri* and the Hawaiian bobtail squid, *Euprymna scolopes*, is a tractable and well-studied model of bacteria-animal mutualism. Here, we developed a method to transiently colonize *E. scolopes* using D-alanine (D-ala) auxotrophy of the symbiont, controlling the persistence of viable infection by supplying or withholding D-ala. We generated alanine racemase (*alr*) mutants of *V. fischeri* that lack avenues for mutational suppression of auxotrophy or reversion to prototrophy. Surprisingly, an Δ*alr* mutant did not require D-ala to grow in a minimal medium, a phenomenon requiring *metC*, which encodes cystathionine β-lyase. Likewise, overexpression of *metC* suppressed D-ala auxotrophy in a rich medium. To block potential mechanisms of suppression, we combined the Δ*alr* mutation with deletions of *metC* and/or *bsrF*, which encodes a broad-spectrum racemase and investigated the suppression rates of four D-ala auxotrophic strains. We then focused on Δ*alr* Δ*bsrF* mutant MC13, which has a suppression rate of $<10^{-9}$. When D-ala was removed from a growing culture of MC13, cells rounded and lysed within 40 minutes. Transient colonization of *E. scolopes* was achieved by inoculating squid in seawater containing MC13 and D-ala, and then transferring the squid into water lacking D-ala, which resulted in loss of viable symbionts within hours. Interestingly, the symbionts within crypt 3 persisted longer than those of crypt 1, suggesting a difference in bacterial growth rate in distinct crypt environments. Our study highlights a new approach for inducing transient colonization and provides insight into the biogeography of the *E. scolopes* light organ.

IMPORTANCE The importance of this study is multi-faceted, providing a valuable methodological tool and insight into the biology of the symbiosis between *Vibrio fischeri* and *Euprymna scolopes*. First, the study sheds light on the critical role of D-ala for bacterial growth, and the underpinnings of D-ala synthesis. Our observations that *metC* obviates the need for D-ala supplementation of an *alr* mutant in minimal medium and that MetC-dependent growth correlates with D-ala in peptidoglycan, corroborate and extend previous findings in *Escherichia coli* regarding a role of MetC in D-ala production. Second, our isolation of robust D-ala auxotrophs led us to a novel method for studying the squid-*Vibrio* symbiosis, allowing for transient colonization without the use of antibiotics, and revealed intriguing differences in symbiont growth parameters in distinct light organ crypts. This work and the methodology developed will contribute to our understanding of the persistence and dynamics of *V. fischeri* within its host.

KEYWORDS *Photobacterium*, *Aliivibrio*, D-alanine, D-amino acids, racemase

The light organ symbiosis between *Vibrio fischeri* and the Hawaiian bobtail squid, *Euprymna scolopes* has been a useful model for understanding the initiation and persistence of beneficial bacterial infections (1–4). *E. scolopes* hatchlings are aposymbiotic, but rapidly acquire *V. fischeri* from their environment (5). *V. fischeri* symbionts live within a specialized bilobed light organ of *E. scolopes*, where they grow and are

Editor Julia C. van Kessel, Indiana University Bloomington, Bloomington, Indiana, USA

Address correspondence to Eric V. Stabb, estabb@uic.edu.

Macey Coppinger and Liu Yang contributed equally to this article. Author order was determined based on duration of involvement in the study.

The authors declare no conflict of interest.

See the funding table on p. 14.

Received 1 July 2024
Accepted 10 August 2024
Published 5 September 2024

bioluminescent (6–8). The host is thought to use the bioluminescence as a camouflaging counter-illumination behavior (9, 10). The animals are inactive during the day, and a large portion of the symbionts are vented from the light organ each dawn, thus increasing *V. fischeri* populations in the environment (11). The light organ is ventral to the ink sac, and is external, constantly in contact with the surrounding seawater (6, 7, 12). Each lobe of the hatchling light organ has a pair of ciliated epithelial appendages (CEAs) that serve to promote infection with *V. fischeri* (13). At the base of each pair of CEAs are three pores, each of which leads to a duct, antechamber, and epithelium-lined crypt. The three crypts are anatomically distinct, with crypt one maturing earliest, and crypt three the latest. Additionally, symbionts of crypt three appear to have slower growth rates, are less likely to be vented, and do not interact in the same ways with epithelial cells as do the bacteria in crypts one and two (14–18).

Studies that initiate and then terminate infections have been useful for understanding host-symbiont dynamics, and for determining whether host responses to infection are reversible. Transient colonization of *E. scolopes* by *V. fischeri* has previously been accomplished by curing infected animals with antibiotics. Chloramphenicol (Cm) was the first used to clear infection early in the symbiosis (19, 20). However, Cm alone proved insufficient for curing a fully established infection, which was achieved by using a combination of Cm and gentamicin (Gm) (21). These studies showed that some developmental programs within *E. scolopes*, including symbiont-induced regression of CEAs, can be irreversibly triggered by transient infection (19), while others, like the behavior of host macrophage-like cells, require persistent presence of *V. fischeri* (21).

While using antibiotics to cure infections has proven useful, there may be drawbacks. Antibiotics must diffuse into host tissues, potentially causing a concentration gradient and uneven exposure. Especially with high drug concentrations, host tissues themselves can be affected by antibiotics (22, 23) or the solvents they are delivered in. Although negative effects on the host have not yet been observed with the Cm and Gm most often used in *V. fischeri-E. scolopes* symbiosis, Cm and Gm have documented off-target effects on Eukaryotic cells (24, 25). Perhaps most importantly, broad-spectrum antibiotics, such as Cm and Gm may also have off-target effects on bacterial symbionts in other organs, such as the gut or accessory nidamental gland (ANG) (26–28). For example, treatment of *E. scolopes* eggs with Cm resulted in fungal infections, presumably by interfering with the bacterial communities transferred to eggs from the maternal ANG, underscoring the possibility of undesirable side effects (26).

An alternative and complementary approach to using antibiotics to generate transient infections is to colonize animals with bacterial mutants that require metabolic supplementation, and then subsequently remove the necessary supplement. For example, bacteria that are auxotrophic for D-ala, D-glutamate (D-glu), and meso-diaminopimelic acid (DAP) colonized mice while being supplemented with these compounds but were cured from the host when these amino acids were no longer provided (29–32). These three amino acids are specific components of the bacterial peptidoglycan (PG) and are not typically found in animals, making it unlikely that hosts could support the growth of auxotrophic strains without external supplementation. However, some auxotrophs can give rise to suppressor mutants that have developed alternative pathways to PG biosynthesis, so mutation of multiple genes or pathways may be required to generate robust auxotrophy (29, 30). These studies led to the goal of developing D-ala auxotrophy of *V. fischeri* to accomplish transient colonization within the *E. scolopes* light organ.

Previously, we reported that an *alr*::mini-Tn*5*-em mutant was auxotrophic for D-ala and unable to colonize *E. scolopes* without D-ala supplementation (33). However, we recently discovered that, despite the lack of an encoded transposase gene, this mini-transposon can precisely be deleted, reverting to the wild-type genotype at the insertion locus (34). We also discovered that rare mutations of *bsrF*, which encodes a broad-spectrum racemase, could compensate for the lack of Alr (34). In this study, we sought to determine whether D-ala auxotrophic strains of *V. fischeri* could be generated that would not give rise to revertants or suppressors, whether such strains could be used to

transiently colonize *E. scolopes*, and if so, what could be learned about the symbiosis from such transient colonization.

RESULTS

To prevent reversion in the *alr*::mini-Tn*5*-em mutant by precise deletion of the transposon, we generated an Δ*alr* mutant (MC6), which is auxotrophic for D-ala in lysogeny broth salts (LBS) medium (Fig. 1). We were initially surprised to discover that the Δ*alr* mutant could grow in a defined minimal medium without D-ala supplementation (Fig. 2), but a hypothetical rationale for the finding was evident from previous studies in *Escherichia coli* (35), as well as our analyses of prototrophic suppressors of MC6, as described below.

To assess the stability of D-ala auxotrophy, we grew MC6 in LBS containing D-ala and then spread the culture to plates without D-ala. The cultures were plated in parallel to LBS with D-ala to determine the number of cells plated and the frequency of suppression. After plating about 10^{10} cells, nine suppressors were generated, for a suppression rate of 9×10^{-10} (Table 1). Genome sequencing revealed that three of the suppressors had mutations in *metG*, which encodes the tRNA synthetase responsible for charging L-met tRNA, while the other six suppressors had mutations in *spoT*, which encodes (p)ppGpp synthetase.

Kang et al. (35) previously showed that upregulation of *metC*, which encodes cystathionine-β-lyase and contributes to L-methionine biosynthesis, restored prototrophic growth to a D-ala auxotrophic *alr dadX* mutant in *E. coli*. We, therefore, considered the possibility that the suppressor mutations in *metG* and *spoT* mimic amino acid (methionine) starvation, and that such mutations lead to increased expression of MetC, and therefore prototrophy in the *alr* mutant.

Consistent with this model, we found that expression of *metC* from a multicopy plasmid in *V. fischeri* compensated for the loss of *alr*, enabling growth on unsupplemented LBS (Fig. 3). Moreover, growth of the Δ*alr* strain in a defined minimal medium without D-ala is dependent on *metC*, although deletion of *metC* also creates L-met auxotrophy (Fig. 2). MetC of *E. coli* can racemize alanine as well as other amino acids, including serine and aminobutyrate (36). To test whether MetC in *V. fischeri* was restoring growth by producing D-ala that is incorporated into PG, we analyzed the amino acid content of PG isolated from the wild-type parent (ES114) and the D-ala auxotroph MC27 (Δ*alr* Δ*metC* Δ*bsrF*) expressing *metC* from a multicopy plasmid. Amino acid analysis of the PG (see Materials and Methods) indicated that both samples have an Ala:DAP:Glu ratio of 2:1:1 that is typical in Gram-negative sacculi. Moreover, they have identical high-performance liquid chromatography (HPLC) chromatograms (Fig. 4), and together these results suggest that MetC is providing D-ala for PG synthesis.

Much like over-expressing *metC*, removing the putative secretion signal of BsrF can compensate for the loss of Alr, obviating the need for D-ala supplementation in the LBS medium (34). Presumably, removing the signal sequence prevents BsrF secretion, trapping BsrF and its racemase activity in the cytoplasm, where Alr racemase activity is normally found. Therefore, to block known possible avenues of D-ala synthesis from L-ala (i.e., genes encoding proteins with alanine racemase activity), we deleted *alr*,

TABLE 1 Selection of prototrophic suppressors of D-ala auxotrophy

	D-alanine suppressor generation					
	Genotype	**CFU plated LBS**	**CFU plated LBS + D-ser**	**Total CFU plated[a]**	**Suppressors**	**Suppressors per CFU**
MC6	Δ*alr*	10^{10}	–[b]	10^{10}	9	9×10^{-10}
MC13	Δ*alr* Δ*bsrF*	6×10^{9}	3×10^{9}	9×10^{9}	0	$<1.1 \times 10^{-10}$
MC24	Δ*alr* Δ*metC*	4.5×10^{9}	–	4.5×10^{9}	0	$<2.2 \times 10^{-10}$
MC27	Δ*alr* Δ*metC* Δ*bsrF*	10^{10}	10^{10}	2×10^{10}	0	$<5 \times 10^{-10}$

[a]For each strain, multiple independent cultures were plated, and the total CFU represents the sum of those multiple biological replicates.
[b]–, cells were not plated on LBS + D-ser.

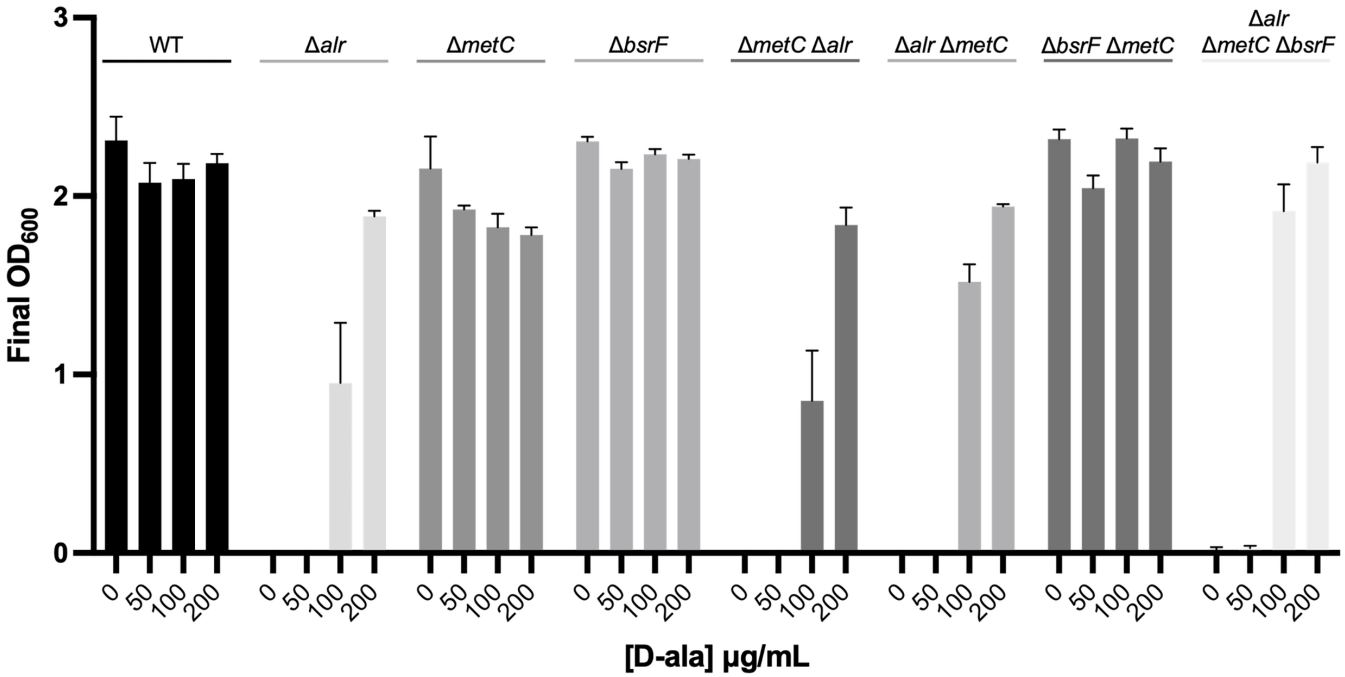

FIG 1 Generation and recovery of D-ala auxotrophy. Shown are the final OD_{600} readings for *V. fischeri* cultures grown in LBS. Cultures were grown for 24 hours before reading the final OD_{600}. Error bars indicate the standard error of the mean ($n = 4$). Data from one representative experiment of at least three is shown.

metC, and *bsrF* singly and in each possible combination (Tables 1 and 2). Similar to MC6, mutants MC13 (Δ*alr* Δ*bsrF*), MC24 (Δ*alr* Δ*metC*), and MC27 (Δ*alr* Δ*metC* Δ*bsrF*), require exogenous D-ala to grow in LBS broth (Fig. 1). All D-ala auxotrophs, regardless of additional mutations beyond deletion of *alr*, required the same concentration of exogenous D-ala, 100 µg/mL, to restore growth in LBS (Fig. 1).

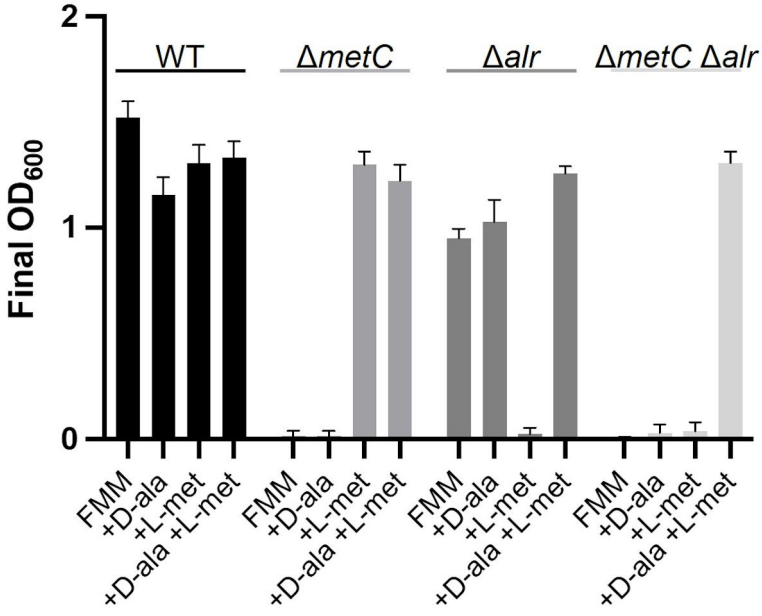

FIG 2 The presence of *metC* in an *alr* mutant enables growth in *Fischeri* minimal medium (FMM) without D-ala supplementation. Strains were grown in minimal media alone, or with 50 µg/mL of D-ala and/or L-met. Strains were grown for 24 hours at 28°C shaking before reading the final OD_{600}. Error bars indicate the standard error of the mean ($n = 3$). Data from one representative experiment of three is shown.

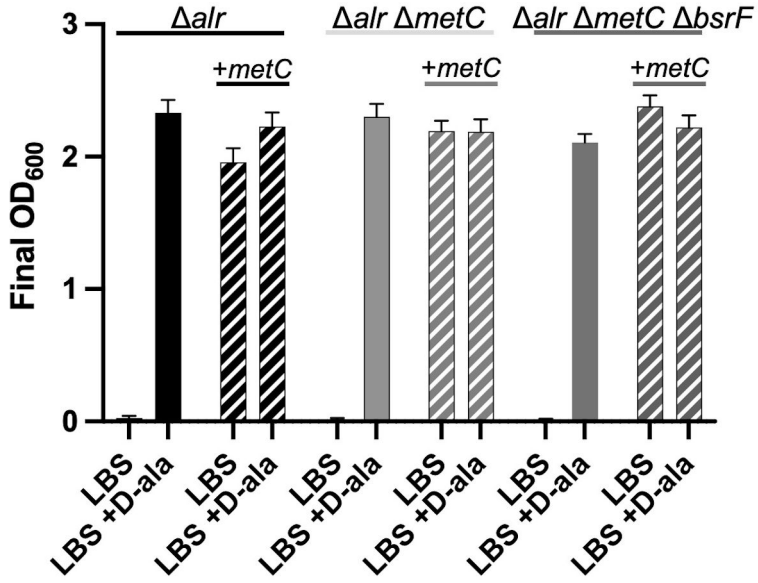

FIG 3 *alr* mutants can be rescued from D-ala auxotrophy by expression of *metC*. Shown are final OD_{600} readings for *V. fischeri* cultures grown in unsupplemented LBS, or LBS supplemented with 200 µg/mL D-ala. Strains include MC6 (Δ*alr*), MC24 (Δ*alr* Δ*metC*), and MC27 (Δ*bsrF* Δ*alr* Δ*metC*) alone, or carrying plasmid pMNC6 (*metC*). Cultures were grown for 24 hours before reading OD_{600}. Error bars indicate the standard error of the mean ($n = 4$). Data from one representative experiment of at least three is shown.

To evaluate the possibility of D-ala prototrophy arising from secondary mutations in *alr* mutants during host colonization, we tested suppression rates in MC13, MC24, and MC27 as we had for MC6 above. For each of these double- or triple-mutant strains, after plating between 4.5×10^9 and 2×10^{10} cells, no prototrophic suppressor mutants were recovered (Table 1). D-serine has previously been found in place of D-ala in some PG (43), and we considered the possibility that if D-ser were present within the squid light organ but not in LBS, it could lead to a higher frequency of suppression in the symbiosis than we had observed in culture. However, after plating $>10^9$ cells of MC13 (Δ*alr* Δ*bsrF*) and MC27 (Δ*alr* Δ*bsrF* Δ*metC*) on LBS supplemented with D-ser, we also failed to isolate suppressors (Table 1). Taken together, our data indicate that for MC13, MC24, and MC27 under the conditions tested, suppression of D-ala auxotrophy appears to occur at a frequency of $<10^{-9}$. For reference, juvenile *E. scolopes* are colonized by approximately 10^5 to 10^6 *V. fischeri* cells.

As illustrated above, deleting *metC* eliminates a potential avenue to D-ala prototrophy, but it isn't clear that the Δ*metC* allele is necessary from a practical standpoint, and the added need for L-met to support growth could complicate symbiotic studies (Fig. 2). Graf and Ruby showed that a methionine auxotroph of *V. fischeri* colonized the light organ at 23% of the population-level achieved by the parent strain at 45 hours post-inoculation (44), suggesting that the host can supply the symbiont with L-met, though perhaps in insufficient quantity to attain full colonization. Although it is possible that the provisioning of L-met is spatially or temporally uneven within host crypts, it seems likely that there is sufficient L-met available for initial colonists, and *metC* may not be highly expressed in this context. Given our observations of *metC*-dependent growth of an *alr* mutant in a minimal medium without D-ala supplementation (Fig. 2), and the fact that intact *metC* did not allow an *alr* mutant to initiate colonization of *E. scolopes* (45), initial symbiont growth in the light organ appears more like growth in LBS than in the defined minimal medium, at least in respect to D-ala metabolism. Given that the likelihood of MetC giving rise to growth without *alr* or exogenous D-ala in the host light organ was relatively low, we proceeded to examine MC13 (Δ*alr* Δ*bsrF*) as a potential tool for initiating and then terminating squid-*Vibrio* symbiosis.

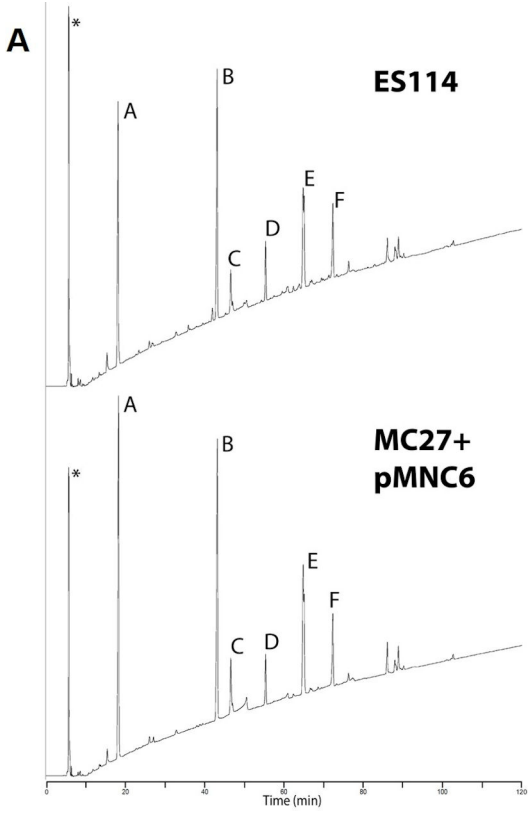

B

Peak	Structure
*	Buffer component
A	DS-TP (Disaccharide tetrapeptide)
B	DS-TP-TP-DS (crosslinked disaccharide-tetrapeptide dimer)
C	anhydroDS-TP (disaccharide tetrapeptide with anhydroNAM)
D	DS-TP-TP-DS-(TP-DS) (crosslinked disaccharide-tetrapeptide trimer)
E	anhydroDS-TP-TP-DS (Crosslinked disaccharide-tetrapeptide dimer with anhydroNAM)
F	Unknown, predicted disaccharide-tetrapeptide trimer with anhydroNAM

FIG 4 MetC rescues D-ala auxotrophy by producing D-ala. (A) HPLC chromatograms of the wild-type parent (ES114; top) and a D-ala auxotroph overexpressing *metC* (bottom; MC27 + pMNC6). ES114 was grown in LBS, while MC27 carrying pMNC6 was grown in LBS-Cm. Peptidoglycan sacculi were purified and digested with Mutanolysin, and muropeptides separated by HPLC, detected by A 206 nm and further analyzed as described previously (37). (B) Identification of labeled peaks in Fig. 4A. * indicates a buffer component peak, while lettered peaks correspond to PG fragments.

We first tested the effect of removing D-ala from pre-grown MC13. The synthesis of PG is essential for maintaining structural integrity and cell morphology (46), and inhibition of PG integrity can result in cell lysis due to increased internal pressure, as is seen with the use of beta-lactam antibiotics (47). We used these observations as a starting point for investigating the response of D-ala auxotrophic *V. fischeri* to a loss of exogenous D-ala. Microscopic observations revealed that depriving MC13 of D-ala led to cells assuming a more rounded form before ultimately rupturing within 40 minutes after D-ala removal (Fig. 5). Such rapid cellular disruption and lethality resulting from D-ala deprivation suggested the potential utility of MC13 as a transient colonizer of *E. scolopes*.

We inoculated juvenile *E. scolopes* overnight with strain MC13, adding 50 µg/mL of D-ala into the filtered seawater (FSW). After overnight inoculation, colonized squid were placed into FSW without D-ala, and maintained for an additional 8 hours, to allow time for D-ala auxotrophic cells within the light organ to outgrow their PG and lyse, as we had observed in culture. The viability of the symbionts within the light organ crypts was evaluated by measuring both luminescence and CFUs (Fig. 6A and B). Initially, both crypts one and three were robustly colonized by MC13, but the removal of D-ala resulted in an absence of detectable symbionts after 24 hours. However, confocal microscopy revealed the persistence of intact MC13 cells in crypt three (Fig. 6C), even though they were not recoverable as CFU (Fig. 6B). Crypt one was largely uncolonized at this point, with the few remaining symbionts exhibiting morphological deviations from the normal bent-rod shape. Forty-eight hours after the removal of D-ala, crypt one continued to show declining levels of bacterial symbionts, while crypt three was still colonized by bent-rod-shaped cells (Fig. 6C). Finally at 72 hours post-D-ala removal, crypt three had

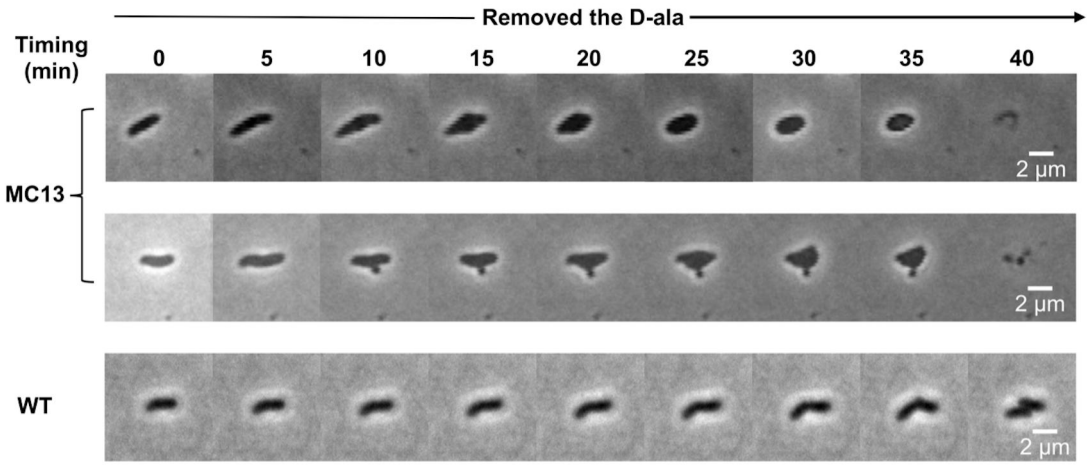

FIG 5 The D-Ala auxotrophic strain of *V. fischeri* requires D-Ala for the maintenance of its PG structure and cellular morphology. Displayed is a time-lapse montage depicting two MC13 cells (top, middle) undergoing morphological degradation and eventual rupture when placed on an agarose pad containing only LBS. Also shown is a time-lapse of a WT (ES114) cell under the same conditions. Images were sequentially acquired every 5 minutes over a 40-minute period.

lost most of its symbiotic *V. fischeri*, and those remaining had assumed the spherical shape typical of dying cells.

DISCUSSION

PG structure is largely conserved across bacteria, due in large part to its structural stability and the D-amino acids that allow it to escape digestion by proteases (48). In most Gram-negative bacteria, the stem peptide consists of L-ala, D-glu, *meso*-DAP, and D-ala (49). In contrast, Gram-positive bacteria usually have L-lysine in the third position (43). Notably, the presence of D-ala at the fourth position of the PG peptide is universally conserved, emphasizing its pivotal role in bacterial cell wall synthesis, as evidenced by the present study.

Alanine racemases can produce the D-ala necessary for PG biosynthesis and are nearly ubiquitous in bacteria. In many species, the primary alanine racemase, often encoded by *alr*, is considered essential for bacterial growth (45, 50–55). However, some bacteria have a secondary source of D-ala as well, which can compensate for the loss of Alr activity (52, 56, 57). Deletion of these alanine racemase-encoding genes leads to D-ala auxotrophy. A study in *E. coli* found that D-ala auxotrophy of an *alr dadX* mutant could be suppressed by overexpression of *metC*, which encodes cystathionine-β-lyase (35), although the PG structure was not analyzed directly, and D-ala production and incorporation were only assumed. Later research of these genes verified that MetC has alanine racemase activity (36, 58). In our study of D-ala auxotrophy and suppression, we also sought to determine if the MetC of *V. fischeri* could play a similar role. We confirmed that in *V. fischeri*, MetC can compensate for D-ala auxotrophy in a defined medium (Fig. 2), and artificial overexpression of MetC can have this effect in a rich medium (Fig. 3). As in *E. coli*, this suppression appears to be due to alanine racemase activity, as evidenced by the presence of D-ala in the PG of a D-ala auxotroph overexpressing *metC*, giving it wild-type PG structure (Fig. 4).

Previously, we identified BsrF, a broad-spectrum racemase that can compensate for the lack of Alr when relegated to the cytoplasmic space of *V. fischeri* (34). To elucidate any remaining potential avenues of D-ala production, we engineered four D-ala auxotrophs and attempted to isolate suppressor mutants of each. Our selection approach parallels previous attempts to evolve PG biosynthesis (34, 37, 59–61). Three such studies found that *m*DAP auxotrophy could be suppressed by the incorporation of lanthionine at the third position of the PG peptide (59–61). Two other studies found that the aspartate

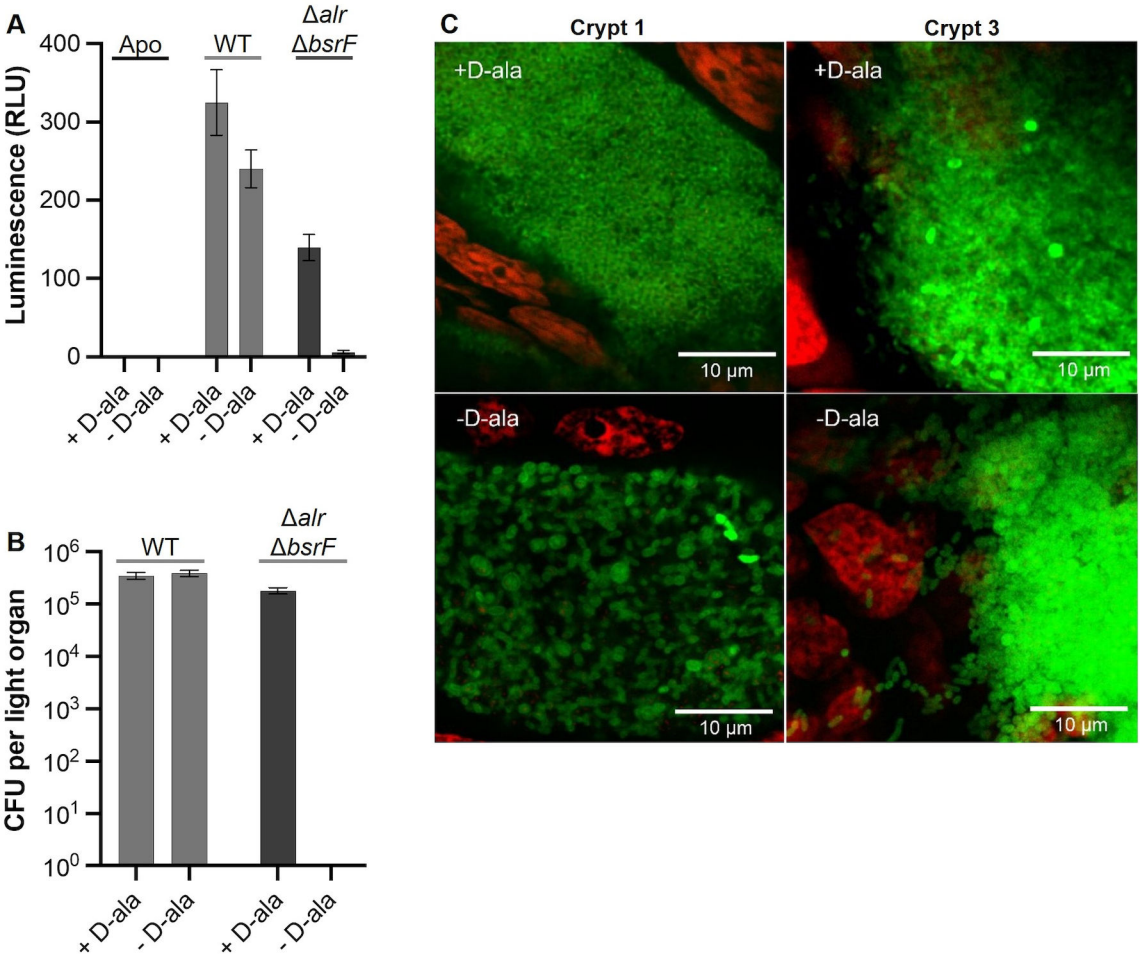

FIG 6 Colonization of *V. fischeri* MC13 in the presence of D-Ala treatment. (A) Animal bioluminescence measured under both aposymbiotic and symbiotic conditions, observed when inoculated with wild type (WT; ES114) or MC13 strains (or no inoculum for aposymbiotic conditions) for 24 hours with 50 µg/mL D-ala treatment. Animal bioluminescence was also assessed 24 hours after D-ala removal. (B) Symbiont population levels (average CFU per light organ) 24 hours post-inoculation for both WT and MC13 strains treated with 50 µg/mL D-ala. Subsequently, the colonized squids were washed and transferred to FSW alone without the addition of D-ala, and symbiont population levels were measured 24 hours thereafter. (C) Representative confocal micrographs of crypts one (left) and three (right) of the light organ colonized for 24 hours by GFP-labeled MC13 strain (carrying pVSV102; refer to Materials and Methods) in FSW with 5 µg/mL D-ala, and visualized 24 hours post-removal of D-ala. Error bars in panels A and B represent standard error (n = 12).

racemase RacD (37) and ΔSS-BsrF (34) could compensate for the loss of glutamate racemase activity by MurI. The latter two studies found suppressors to have wild-type PG structure, implicating the racemases as having glutamate racemase activity. Based on these previous studies, as well as the current work, it appears that D-glu and D-ala may be more difficult moieties to replace in PG than *m*DAP.

Previous studies have used PG-specific D-amino acid auxotrophs as transient colonizers of cell cultures (62) and mice (29, 30), and even as vaccines against bacterial pathogens (31, 63, 64). Currently, transient colonization of *E. scolopes* is accomplished by the use of antibiotics (19–21). Here, we employed the use of *V. fischeri* strains auxotrophic for a PG-specific D-amino acid instead.

Upon supplying D-ala in the seawater, the MC13 (Δ*alr* Δ*bsrF*) D-ala auxotroph was able to colonize hatchling *E. scolopes* (Fig. 6). When D-ala is removed from growth medium, the auxotrophic bacteria rapidly begin to lose their normal cell morphology before finally lysing (Fig. 5), and similarly, removal of D-ala from the seawater results in transient colonization of the squid (Fig. 6). Understanding the dynamics of host-microbe interactions is especially crucial during the early, stress-susceptible stages of life, as

organisms enter the environment and acquire their microbiomes. The deployment of auxotrophic strains unveils a complementary methodology to specifically target the growth dynamics of one species without perturbing the equilibrium of an entire microbiome, including the microbial communities found in the adult *E. scolopes* gut and ANG. The different modes of action of treating with bacteriostatic antibiotics such as chloramphenicol or inducing lysis by depriving cells of D-ala may also have different outcomes based on how the symbionts die and degrade, and accordingly, these approaches may be further viewed as complementary and corroborative. In sum, the approach described should prove useful for long-term studies of the effects of cleared colonization of the light organ.

Studies of transient bacterial infections can inform our understanding of host-microbe dynamics, and specifically, this research can aid in understanding the intricacies of symbiont-induced host maturation. For example, this method provided additional information about the distinct biogeographies of the three crypt spaces within the *E. scolopes* light organ. Previous studies have shown that crypt three is the last to form and has distinct chemical and morphological differences from crypts one and two (14–18). The present research underscores the differences of this crypt, as we observed the symbionts of crypt three to outlast those in crypt one after removal of D-ala from the seawater (Fig. 6). Although D-ala levels were not measured in the crypts over time, crypt-specific diffusion or exclusion of other small molecules (e.g., stains), has not been reported.

We speculate that symbionts within crypt three grow more slowly than those in the other crypts, allowing them to prolong their stores of D-ala longer than symbionts of crypts one and two. In support of this model, a recent study in *V. fischeri* utilized fluorescent D-ala derivatives that incorporate into growing PG, concluding that symbionts in crypt 3 have less growth reflected in new PG synthesis than those in crypt 1 (65). Additionally, crypt three appears to be vented less often than the others (17), leaving a greater number of symbionts inside, regardless of growth rate.

Understanding the factors that contribute to this variability in crypt development and symbiont colonization could shed light on the selective pressures and adaptive strategies employed by both hosts and symbionts, and strengthen previous hypotheses that the less-mature crypt three acts as a sanctuary, potentially safeguarding the symbionts from stress, i.e., antibiotic treatment (17, 18), or nutrient limitation. The use of D-ala auxotrophs should be a useful tool for further investigating these dynamics in the model *V. fischeri-E. scolopes* symbiosis.

MATERIALS AND METHODS

Bacterial strains and culture conditions

The strains and plasmids used in this study are listed in Table 2. When added to LB medium (66) for selection of *E. coli*, Cm and kanamycin (Km) were used at concentrations of 20 and 40 µg/mL, respectively. For the selection of *E. coli* with Em, 150 µg/mL was added to the BHI medium (Difco, Sparks, MD). When added to LBS (67) for selection of *V. fischeri*, Cm, Em, and Km were used at concentrations of 2, 5, and 100 µg/mL, respectively. In LBS, D-ala was added at a final concentration of 400 µg/mL for auxotrophic strains unless otherwise indicated. *Fischeri* minimal medium (FMM) [1 mM Tris (pH 7.5), 400 mM NaCl, 10 mM KCl, 50 mM $MgSO_4$, 10 mM $CaCl_2$, 2 µM $FeSO_4$, 2 mM glycerol-3-phosphate, 5 mM ribose, 20 mM NAG] was used to pre-grow cells for natural transformation of *V. fischeri*. In FMM, D-ala was added at a final concentration of 100 µg/mL. Agar was added to a final concentration of 1.5% for solid media.

Molecular genetics and sequence analysis

The plasmids used in this study are listed in Table 2. Oligonucleotides used for PCR and cloning are listed in Table 3 and were synthesized by Integrated DNA Technologies (Coraville, IA). DNA ligase and restriction enzymes were purchased from New England

TABLE 2 Strains used in this study[a]

Strain	Genotype	Source
E. coli		
DH5α	φ80d*lacZ*ΔM15 Δ(*lacZYA-argF*)U169 *deoR supE44 hsdR17 recA1 endA1 gyrA96 thi-1 relA1*	(38)
DH5αλ*pir*	DH5α lysogenized with λpir	(39)
CC118λ*pir*	***Δ***(*ara-leu*) *araD* ***Δ****lac74 galE galK phoA20 thi-1 rpsE rpsB argE*(Am) *recA* λ*pir*	(40)
V. fischeri		
AKD100	ES114 with a mini-Tn*7*-Em	(41)
ES114	Wild-type isolates from *E. scolopes*	(42)
KL3	Δ*bsrF*	(34)
MC2	Δ*metC*::FRT-Em^{R}	This study
MC3	Δ*alr*::FRT-Em^{R}	This study
MC5	Δ*metC*::FRT	This study
MC6	Δ*alr*::FRT	This study
MC6S01	Δ*alr*::FRT *spoT*^{C1370T}	This study
MC6S02	Δ*alr*::FRT *spoT*^{G1046T} *spoT*^{G1049T}	This study
MC6S03	Δ*alr*::FRT *spoT*^{A1053C} *spoT*^{A1058G}	This study
MC6S04	Δ*alr*::FRT *metG*^{A1159G}	This study
MC6S05	Δ*alr*::FRT *spoT*^{A1053C} *spoT*^{A1058G}	This study
MC6S06	Δ*alr*::FRT *metG*^{C1148A}	This study
MC6S07	Δ*alr*::FRT *spoT*^{C818T}	This study
MC6S08	Δ*alr*::FRT *spoT*^{A1058G} *spoT*^{AGC1051CAG}	This study
MC6S09	Δ*alr*::FRT *metG*^{C32A}	This study
MC8	Δ*bsrF* Δ*metC*::FRT-Em^{R}	This study
MC12	Δ*bsrF* Δ*metC*::FRT	This study
MC13	Δ*bsrF* Δ*alr*::FRT	(34)
MC23	Δ*alr*::FRT Δ*metC*::FRT-Em^{R}	This study
MC24	Δ*alr*::FRT Δ*metC*::FRT	This study
MC26	Δ*bsrF* Δ*alr*::FRT Δ*metC*::FRT-Em^{R}	This study
MC27	Δ*bsrF* Δ*alr*::FRT Δ*metC*::FRT	This study

[a]Drug resistance abbreviation used: em, erythromycin; cm, chloramphenicol, Km, kanamycin.

Biolabs (Beverly, MA). PCR for chromosomal deletion by transformation was conducted with KOD DNA polymerase (Millipore Sigma, Burlington, MA). PCR for plasmid cloning was conducted with Phusion DNA polymerase (New England Biolabs). Plasmids used for cloning were prepared with the ZymoPURE Plasmid Miniprep kit (Zymo Research, Irvine, CA). DNA was repurified after PCR and between cloning steps using the DNA Clean & Concentrator kit from Zymo Research. Plasmid inserts were Sanger sequenced at the University of Michigan Advanced Genomics core facility (Ann Arbor, MI). gDNA from *V. fischeri* strains was extracted using the Invitrogen PureLink Genomic DNA Mini Kit (Thermo Fisher Scientific, Inc.) and used as a template for PCR. For whole-genome sequencing, strains were grown overnight then pelleted, and sent to SeqCoast Genomics (Portsmouth, NH, USA) to perform DNA extraction, and strain-typing via Illumina sequencing. All sequences were analyzed via Geneious Prime with default settings, compared to *V. fischeri* wild-type strain ES114. Paired-end reads were mapped to the reference, then single-nucleotide polymorphisms were identified with a minimum variant frequency of 0.8.

Plasmid construction

Plasmids were maintained in *E. coli* DH5α, with the exception of pVSV105 and its derivatives which were maintained in DH5αλpir, and pEVS104 which was maintained in CC118*λpir* (40). When relevant, plasmids were conjugated into *V. fischeri* via triparental mating with helper plasmid pEVS104. Complementation plasmid pMNC6 was constructed by amplifying *metC* from ES114 with primers MNC7 and MNC8. This PCR product

TABLE 3 Plasmids and primers used in this study

Plasmid[a]	Relevant characteristics	Source
pCR-Blunt II-TOPO	$oriV_{ColE1}$, km^R	Thermo Fisher
pEVS104	Conjugative helper plasmid; $oriV_{R6K}$ $oriT_{RP4}$ km^R	(40)
pEVS118	*ori*VR6K *ori*TRP4, cm^R	(39)
pKAL4	*bsrF* from ES114 cloned into pCR-Blunt II-TOPO	(34)
pKAL6	*bsrF* from ES114 cloned into pVSV105	(34)
pKV494	pJET + FRT-Em^R	(68)
pKV496	pEVS79-Kn^R + flp^+	(68)
plostfoX	$tfoX^+$, Cm^R	(69)
pMNC4	*metC* from ES114 cloned into pCR-Blunt II-TOPO	This study
pMNC6	*metC* from ES114 cloned into pVSV105	This study
pMNC26	Δ*SS-bsrF* cloned from pKAL6 into pVSV105	(34)
pVSV102	Km^R, *gfp*	(15)

Primer[b]	Sequence	Source
Frt-F	CCATACTTAGTGCGGCCGCCTA	(68)
Frt-R	CCATGGCCTTCTAGGCCTATCCC	(68)
MNC7	CAT GCT AGC ACT AGT GAA TGG ATT CAT ATG	This study
MNC8	CAT GCT AGC CGC CTT TAA TTT ATT GTT AAG	This study
MNC39	GAT CTA AGA CAA AAA CTG CAA TAA GG	This study
MNC40	taggcggccgcactaagtatgg CAT ATG AAT CCA TTC AAT AAA AAG	This study
MNC41	ggataggcctagaaggccatgg TAACAATAAATTAAAGGCGATATT	This study
MNC42	CATCAATCTGGATAAGACGAACGC	This study
MNC51	GGGCTCGTATTTCTTCTACTATGGGC	(34)
MNC52	taggcggccgcactaagtatggCATGATTCAGCCTTATTATTCATCA	(34)
MNC53	ggataggcctagaaggccatggAATGAGAGTCTTCTTGAATTCATT	(34)
MNC54	CTCTATACTCGAGACACCGCTATC	(34)

[a]Alleles cloned in this study are from *V. fischeri* strain ES114. Replication origins (*oriV*) on each vector are listed as R6K and/or ColE1. Plasmids based on pES213 are stable in *V. fischeri* and do not require antibiotic selection for maintenance (15).
[b]All oligonucleotides are shown in the 5′-to-3′ direction. Lowercase bases represent the tail sequences used for splicing fragments via SOE PCR.

was cloned into pCR-Blunt II TOPO (Thermo Fisher, Waltham, MA), yielding pMNC4. pMNC4 was then digested with NheI, and the *metC*-containing fragment was ligated into XbaI-cut pVSV105 (40), producing pMNC6.

Construction of mutant strains

For all mutant strains engineered in this study, chromosomal deletions in ES114 were created via overlap extension PCR (SOE-PCR), by generating mutant alleles, which were introduced by TfoX-mediated transformation (69). An Em-resistance cassette flanked by Frt-recombinase recognition sites was amplified with KOD DNA polymerase from plasmid pKV494 using primers Frt-F and Frt-R (68). Deletions of *metC* and *alr* were made by splicing fragments from upstream and downstream of the genes to the Em resistance cassette by SOE-PCR (68). Briefly, a ~500 bp fragment upstream of *metC* was amplified from ES114 using primers MNC39 and MNC40, and the ~500 bp region downstream of *metC* was amplified using primers MNC41 and MNC42. The ~500 bp region upstream of *alr* was amplified from ES114 using primers MNC51 and MNC52, and the ~500 bp region downstream of *alr* was amplified using primers MNC53 and MNC54. These pairs of flanking sequences were fused to the Em-Frt cassette by SOE-PCR, and the resulting deletion-allele fragments were then transformed into *V. fischeri* strains harboring the TfoX-overexpressing plasmid plosTfoX (69). Strains were then selected on LBS containing Em (and D-ala, for Δ*alr* strains). The Em cassette was removed from each mutant via *flp* recombinase expression on pKV496 to leave an FLP recognition-site scar, and finally, the FLP-expressing plasmid was cured (68). The Δ*metC* allele was then verified in resulting

strains by PCR amplification with primers MNC39 and MNC41, and the Δ*alr* allele was verified with primers MNC51 and MNC54. Strain MC2 was generated by replacing *metC* in ES114 with the Δ*metC*-Em deletion fragment. Removal of the Em cassette generated strain MC5. Strain MC3 was generated by replacing *alr* in ES114 with the Δ*alr*-Em deletion fragment. Removal of the Em cassette generated strain MC6. Strain MC8 was generated from KL3 (34) by replacing *metC* with the Δ*metC*-Em deletion fragment. Removal of the Em cassette generated strain MC12. Strain MC23 was generated from MC6 by replacing *metC* with the Δ*metC*-Em deletion fragment. Removal of the Em cassette generated strain MC24. Strain MC26 was generated from MC13 (34) by replacing *metC* with the Δ*metC*-Em deletion fragment. Removal of the Em cassette generated strain MC27.

Selection of spontaneous suppressors of D-ala auxotrophy

D-ala auxotrophs (MC6, MC13, MC24, and MC27) were grown in LBS containing 400 µg/mL D-ala to an OD_{600} of 1. Aliquots of 100 µL taken from multiple independent cultures were plated to LBS without D-ala. Cultures were dilution-plated in parallel on LBS with D-ala, to determine the number of CFU plated, thereby enabling calculation of mutation frequency. Plates were incubated at 28°C, and colonies were counted at 24 and 48 hours post-inoculation. Suppressor colonies were streak-purified, then grown in LBS without D-ala supplementation, and stocked at −80°C in 20% glycerol.

Analysis of PG amino acid and muropeptide content

Cells were grown overnight in LBS (or LBS-Cm), chilled on ice for 10 minutes, and centrifuged at 4°C and 17,600 × *g* for 15 minutes. Pellets were resuspended in 10 mL water that had been chilled on ice, then dripped into 50 mL of boiling 4% SDS. The solution was boiled for 30 minutes with continuous stirring and allowed to cool to room temperature, at which point they were centrifuged at 120,000 × *g* for 60 minutes, resuspended in room temperature water, and washed three to four more times by centrifugation and resuspension as above. Before resuspension, the supernatant was assayed for SDS using methylene blue and chloroform (70) and washed repeatedly until no SDS was detected. When SDS was undetectable, the pellet was resuspended in 1 mL of water, then treated with 10 µg DNase I and 50 µg RNase A for 2 hours at 37°C. Samples were then treated with 100 µg of Trypsin, and $CaCl_2$ was added to a final concentration of 10 mM. Samples were then incubated overnight at 37°C, and then centrifuged at 15,880 × *g* for 10 minutes, after which pellets were resuspended in 1% SDS. The solution was incubated in a 95°C hot water bath for 20 minutes, diluted into warm water, and then centrifuged at 120,000 × *g* for 60 minutes at room temperature. The pellet was then washed with warm water and centrifuged as above, until SDS-free. Subsequent pellets were then resuspended in 12.5 mM $NaPO_4$ (pH 5.5) and digested with 125 units of Mutanolysin at 37°C overnight. Insoluble material was removed by centrifugation at 15,880 × *g* for 15 minutes. The muropeptide-containing supernatant was transferred to a new tube, lyophilized until dry, and stored at −20°C until analysis. The mixture of muropeptides was subjected to amino acid analysis in comparison to known standards (71) and HPLC muropeptide separation (72) as previously described.

Time-lapse microscopy of D-ala auxotrophic bacteria

Wild type and MC13 were initially cultured at 28°C in an LBS medium; MC13 was supplemented with 400 µg/mL of D-ala. Cultures were grown until the bacterial population reached an exponential phase, with OD_{600} between 0.4 and 0.8. Cells were harvested by centrifugation at 7,000 × *g* for 1 minute at room temperature, then resuspended in LBS without D-ala supplementation. A 1 µL aliquot of cells was carefully placed onto a pad containing 1.0% agarose in LBS and sealed with a coverslip. Time-lapse images were captured at 5-minute intervals over a period of 2 hours, by an inverted Zeiss LSM 980 microscope equipped with a Plan Apochromat 1.4NA 100× oil Phase 3 objective at the Caltech Biological Imaging Facility. The acquired time-lapse sequences

were subsequently processed and visualized in ImageJ, enabling the generation of a comprehensive image montage.

Squid colonization assay

V. fischeri ES114 was cultured overnight at 28°C in LBS medium, and D-ala auxotrophic strain MC13 carrying *gfp*-expressing plasmid pVSV102 was grown in LBS with 400 µg/mL of D-ala and 100 µg/mL km for plasmid retention. Overnight cultures were diluted 100-fold into Seawater Tryptone liquid medium and allowed to grow until mid-exponential phase at 28°C, then diluted to a final inoculum concentration of ~5,000 CFU/mL in 100 mL of FSW. ES114 was inoculated into FSW alone, while MC13 was supplemented with 5 µg/mL D-ala. Newly hatched *E. scolopes* were introduced into these mixtures and allowed to colonize overnight under a 12/12 hour day-night cycle. Animals from different egg clutches were used to minimize the chance of an unusual clutch-specific (e.g., genetic) variation leading to anomalous results, and hatchlings from different clutches were evenly distributed across the treatments. After about 16 hours, the squid was transferred into individual vials with fresh FSW. ES114-inoculated squid were placed into FSW; half of the MC13-inoculated squid were transferred into FSW alone, while the other half were transferred into FSW supplemented with 5 µg/mL D-ala. At 24 hours post-inoculation, luminescence was measured using a TD 20/20 luminometer (Turner Designs, Sunnyvale, CA), after which the squid was either transferred to fresh FSW with D-ala as needed or frozen at −80°C in 700 µL of FSW until ready for use. Most squid were individually homogenized and then diluted in an LBS agar medium diluted in LBS broth and spread to LBS plates, and the number of CFU/mL was determined. Five squids from each treatment (D-ala or no D-ala) were fixed in 4% paraformaldehyde (PFA) solution in 1× marine PBS (mPBS) for microscopy, as previously described (18).

Light microscopy and fluorescence imaging

PFA-fixed juvenile *E. scolopes* were dissected, treated with TO-PRO-3 Iodide (Thermo Fisher Scientific) to stain nuclei, and permeabilized overnight in 0.1% Triton X-100 in mPBS (mPBST). The squid wereas washed in mPBST for 15 minutes and then mounted in Vectashield (Vector Laboratories, Burlingame, CA) for imaging. Imaging was conducted using a Zeiss LSM 980 confocal microscope equipped with a Zeiss Plan Apochromat 1.4NA 63× oil objective lens at the Caltech Biological Imaging Facility.

ACKNOWLEDGMENTS

This work was supported by the NSF grant IOS-1557964 awarded to E.V.S. and D.L.P.

We would like to thank the Caltech Biological Imaging Center where we performed the microscopy imaging.

AUTHOR AFFILIATIONS

[1]Department of Microbiology, University of Georgia, Athens, Georgia, USA
[2]Department of Biological Sciences, University of Illinois at Chicago, Chicago, Illinois, USA
[3]Division of Biosphere Sciences and Engineering, California Institute of Technology, Pasadena, California, USA
[4]Department of Biological Sciences, Virginia Tech, Blacksburg, Virginia, USA

AUTHOR ORCIDs

Macey Coppinger http://orcid.org/0000-0002-0743-873X
David L. Popham http://orcid.org/0000-0002-2614-143X
Eric V. Stabb http://orcid.org/0000-0001-7000-4275

FUNDING

Funder	Grant(s)	Author(s)
National Science Foundation (NSF)	IOS-1557964	David L Popham Eric V. Stabb

AUTHOR CONTRIBUTIONS

Macey Coppinger, Conceptualization, Investigation, Methodology, Writing – original draft, Writing – review and editing | Liu Yang, Conceptualization, Investigation, Methodology, Project administration, Supervision, Visualization, Writing – review and editing | Edward Ruby, Methodology, Project administration, Supervision, Writing – review and editing | Eric V. Stabb, Conceptualization, Investigation, Methodology, Project administration, Supervision, Visualization, Writing – review and editing.

DATA AVAILABILITY

Illumina reads from whole-genome sequencing of ES114, MC6, and the nine MC6 suppressors are available in NCBI's Sequence Read Archive (SRA) within Bioproject PRJNA1078398 under accession numbers SAMN39999377 through SAMN39999387. All other raw and derived data supporting the findings of this study are available from the corresponding author, E.V.S., upon request.

REFERENCES

1. Stabb EV. 2006. The *Vibrio fischeri-Euprymna scolopes* light organ symbiosis, p 204–218. In Thompson FL, Austin B, Swings J (ed), The Biology of Vibrios. ASM Press, Washington, DC.
2. Stabb EV, Visick KL. 2013. *Vibrio fischeri*: a bioluminescent light-organ symbiont of the bobtail squid *Euprymna scolopes*, p 497–532. In EF Delong, S Lory, E Stackebrandt, F Thompson (ed), The prokaryotes: prokaryotic biology and symbiotic associations, Fourth. Springer.
3. Nyholm SV, McFall-Ngai MJ. 2021. A lasting symbiosis: how the Hawaiian bobtail squid finds and keeps its bioluminescent bacterial partner. Nat Rev Microbiol 19:666–679. https://doi.org/10.1038/s41579-021-00567-y
4. Visick KL, Stabb EV, Ruby EG. 2021. A lasting symbiosis: how *Vibrio fischeri* finds a squid partner and persists within its natural host. Nat Rev Microbiol 19:654–665. https://doi.org/10.1038/s41579-021-00557-0
5. Wei SL, Young RE. 1989. Development of symbiotic bacterial bioluminescence in a nearshore cephalopod, *Euprymna scolopes*. Mar Biol 103:541–546.
6. Kishitani T. 1928. Ueber das Leuchtorgan von *Euprymna morsei* Verrill und die symbiotischen Leuchtbakterien. Proc Imp Acad 4:306–309. https://doi.org/10.2183/pjab1912.4.306
7. Ruby EG, McFall-Ngai MJ. 1992. A squid that glows in the night: development of an animal-bacterial mutualism. J Bacteriol 174:4865–4870. https://doi.org/10.1128/jb.174.15.4865-4870.1992
8. Nyholm SV, Stabb EV, Ruby EG, McFall-Ngai MJ. 2000. Establishment of an animal-bacterial association: recruiting symbiotic *Vibrios* from the environment. Proc Natl Acad Sci U S A 97:10231–10235. https://doi.org/10.1073/pnas.97.18.10231
9. Jones BW, Nishiguchi MK. 2004. Counterillumination in the Hawaiian bobtail squid, *Euprymna scolopes* Berry (Mollusca: Cephalopoda). Mar Biol 144:1151–1155. https://doi.org/10.1007/s00227-003-1285-3
10. Stabb EV, Millikan DS. 2009. Is the *Vibrio fischeri-Euprymna scolopes* symbiosis a defensive mutualism?, p 103–116. In Defensive mutualism in microbial symbiosis. CRC Press.
11. Boettcher KJ, Ruby EG, McFall-Ngai MJ. 1996. Bioluminescence in the symbiotic squid *Euprymna scolopes* is controlled by a daily biological rhythm. J Comp Physiol A 179:65–73. https://doi.org/10.1007/BF00193435
12. McFall-Ngai MJ, Montgomery MK. 1990. The anatomy and morphology of the adult **b**acterial light organ of *Euprymna scolopes* Berry (Cephalopoda:Sepiolidae). Biol Bull 179:332–339. https://doi.org/10.2307/1542325
13. Montgomery MK, McFall-Ngai M. 1993. Embryonic development of the light organ of the sepiolid squid *Euprymna scolopes* Berry. Biol Bull 184:296–308. https://doi.org/10.2307/1542448
14. McFall-Ngai MJ, Ruby EG. 1998. Sepiolids and *Vibrios*: when first they meet. Bioscience 48:257–265. https://doi.org/10.2307/1313352
15. Dunn AK, Millikan DS, Adin DM, Bose JL, Stabb EV. 2006. New rfp- and pES213-derived tools for analyzing symbiotic *Vibrio fischeri* reveal patterns of infection and lux expression *in situ*. Appl Environ Microbiol 72:802–810. https://doi.org/10.1128/AEM.72.1.802-810.2006
16. Sycuro LK, Ruby EG, McFall-Ngai M. 2006. Confocal microscopy of the light organ crypts in juvenile *Euprymna scolopes* reveals their morphological complexity and dynamic function in symbiosis. J Morphol 267:555–568. https://doi.org/10.1002/jmor.10422
17. Essock-Burns T, Bongrand C, Goldman WE, Ruby EG, McFall-Ngai MJ. 2020. Interactions of symbiotic partners drive the development of a complex biogeography in the squid-*Vibrio* symbiosis. MBio 11:e00853-20. https://doi.org/10.1128/mBio.00853-20
18. Essock-Burns T, Lawhorn S, Wu L, McClosky S, Moriano-Gutierrez S, Ruby EG, McFall-Ngai MJ. 2023. Maturation state of colonization sites promotes symbiotic resiliency in the *Euprymna scolopes-Vibrio fischeri* partnership. Microbiome 11:68. https://doi.org/10.1186/s40168-023-01509-x
19. Doino JA, McFall-Ngai MJ. 1995. A transient exposure to symbiosis-competent bacteria induces light organ morphogenesis in the host squid. Biol Bull 189:347–355. https://doi.org/10.2307/1542152
20. Lamarcq LH, McFall-Ngai MJ. 1998. Induction of a gradual, reversible morphogenesis of its host's epithelial brush border by *Vibrio fischeri*. Infect Immun 66:777–785. https://doi.org/10.1128/IAI.66.2.777-785.1998
21. Nyholm SV, Stewart JJ, Ruby EG, McFall-Ngai MJ. 2009. Recognition between symbiotic *Vibrio fischeri* and the haemocytes of *Euprymna scolopes*. Environ Microbiol 11:483–493. https://doi.org/10.1111/j.1462-2920.2008.01788.x
22. MacDonald ML, Lamerdin J, Owens S, Keon BH, Bilter GK, Shang Z, Huang Z, Yu H, Dias J, Minami T, Michnick SW, Westwick JK. 2006. Identifying off-target effects and hidden phenotypes of drugs in human cells. Nat Chem Biol 2:329–337. https://doi.org/10.1038/nchembio790
23. Campillos M, Kuhn M, Gavin AC, Jensen LJ, Bork P. 2008. Drug target identification using side-effect similarity. Science 321:263–266. https://doi.org/10.1126/science.1158140
24. Elliott RL, Jiang X-P. 2019. The adverse effect of gentamicin on cell metabolism in three cultured mammary cell lines: "Are cell culture data

skewed?" PLOS ONE 14:e0214586. https://doi.org/10.1371/journal.pone.0214586
25. Nozaka A, Nishiwaki A, Nagashima Y, Endo S, Kuroki M, Nakajima M, Narukawa M, Kamisuki S, Arazoe T, Taguchi H, Sugawara F, Kamakura T. 2019. Chloramphenicol inhibits eukaryotic Ser/Thr phosphatase and infection-specific cell differentiation in the rice blast fungus. Sci Rep 9:9283. https://doi.org/10.1038/s41598-019-41039-x
26. Kerwin AH, Gromek SM, Suria AM, Samples RM, Deoss DJ, O'Donnell K, Frasca S, Sutton DA, Wiederhold NP, Balunas MJ, Nyholm SV. 2019. Shielding the next generation: symbiotic bacteria from a reproductive organ protect bobtail squid eggs from fungal fouling. MBio 10:e02376-19. https://doi.org/10.1128/mBio.02376-19
27. Kerwin AH, McAnulty SJ, Nyholm SV. 2021. Development of the accessory nidamental gland and associated bacterial community in the Hawaiian Bobtail squid, *Euprymna scolopes* Biol Bull 240:205–218. https://doi.org/10.1086/713965
28. McAnulty SJ, Kerwin AH, Koch E, Nuttall B, Suria AM, Collins AJ, Schleicher TR, Rader BA, Nyholm SV. 2023. "Failure to launch": development of a reproductive organ linked to symbiotic bacteria. MBio 14:e0213122. https://doi.org/10.1128/mbio.02131-22
29. Hapfelmeier S, Lawson MAE, Slack E, Kirundi JK, Stoel M, Heikenwalder M, Cahenzli J, Velykoredko Y, Balmer ML, Endt K, Geuking MB, Curtiss R 3rd, McCoy KD, Macpherson AJ. 2010. Reversible microbial colonization of germ-free mice reveals the dynamics of IgA immune responses. Science 328:1705–1709. https://doi.org/10.1126/science.1188454
30. Cuenca M, Pfister SP, Buschor S, Bayramova F, Hernandez SB, Cava F, Kuru E, Van Nieuwenhze MS, Brun YV, Coelho FM, Hapfelmeier S. 2016. D-alanine-controlled transient intestinal mono-colonization with non-laboratory-adapted commensal *E. coli* strain HS. PLoS One 11:e0151872. https://doi.org/10.1371/journal.pone.0151872
31. Moscoso M, García P, Cabral MP, Rumbo C, Bou G. 2018. A D-alanine auxotrophic live vaccine is effective against lethal infection caused by *Staphylococcus aureus*. Virulence 9:604–620. https://doi.org/10.1080/21505594.2017.1417723
32. Cabral MP, García P, Beceiro A, Rumbo C, Pérez A, Moscoso M, Bou G. 2017. Design of live attenuated bacterial vaccines based on D-glutamate auxotrophy. Nat Commun 8:15480. https://doi.org/10.1038/-ncomms15480
33. Lyell NL, Dunn AK, Bose JL, Vescovi SL, Stabb EV. 2008. Effective mutagenesis of *Vibrio fischeri* by using hyperactive mini-Tn5 derivatives. Appl Environ Microbiol 74:7059–7063. https://doi.org/10.1128/AEM.01330-08
34. Coppinger MN, Laramore K, Popham DL, Stabb EV. 2024. A prototrophic suppressor of a *Vibrio fischeri* D-glutamate auxotroph reveals a member of the periplasmic broad-spectrum racemase family (BsrF). J Bacteriol 206:e0033323. https://doi.org/10.1128/jb.00333-23
35. Kang L, Shaw AC, Xu D, Xia W, Zhang J, Deng J, Wöldike HF, Liu Y, Su J. 2011. Upregulation of MetC is essential for D-alanine-independent growth of an alr/dadX-deficient *Escherichia coli* strain. J Bacteriol 193:1098–1106. https://doi.org/10.1128/JB.01027-10
36. Miyamoto T, Katane M, Saitoh Y, Sekine M, Homma H. 2018. Cystathionine β-lyase is involved in D-amino acid metabolism. Biochem J 475:1397–1410. https://doi.org/10.1042/BCJ20180039
37. Jones RM, Popham DL, Schmidt AL, Neidle EL, Stabb EV. 2018. *Vibrio fischeri* DarR directs responses to D-aspartate and represents a group of similar LysR-type transcriptional regulators. J Bacteriol 200:e00773-17. https://doi.org/10.1128/JB.00773-17
38. Hanahan D. 1983. Studies on transformation of *Escherichia coli* with plasmids. J Mol Biol 166:557–580. https://doi.org/10.1016/s0022-2836(83)80284-8
39. Dunn AK, Martin MO, Stabb EV. 2005. Characterization of pES213, a small mobilizable plasmid from *Vibrio fischeri*. Plasmid 54:114–134. https://doi.org/10.1016/j.plasmid.2005.01.003
40. Stabb EV, Ruby EG. 2002. RP4-based plasmids for conjugation between *Escherichia coli* and members of the Vibrionaceae. Meth Enzymol 358:413–426. https://doi.org/10.1016/s0076-6879(02)58106-4
41. Septer AN, Wang Y, Ruby EG, Stabb EV, Dunn AK. 2011. The haem-uptake gene cluster in *Vibrio fischeri* is regulated by Fur and contributes to symbiotic colonization. Environ Microbiol 13:2855–2864. https://doi.org/10.1111/j.1462-2920.2011.02558.x
42. Boettcher KJ, Ruby EG. 1990. Depressed light emission by symbiotic *Vibrio fischeri* of the sepiolid squid *Euprymna scolopes*. J Bacteriol 172:3701–3706. https://doi.org/10.1128/jb.172.7.3701-3706.1990
43. Vollmer W, Blanot D, de Pedro MA. 2008. Peptidoglycan structure and architecture. FEMS Microbiol Rev 32:149–167. https://doi.org/10.1111/j.1574-6976.2007.00094.x
44. Graf J, Ruby EG. 1998. Host-derived amino acids support the proliferation of symbiotic bacteria. Proc Natl Acad Sci U S A 95:1818–1822. https://doi.org/10.1073/pnas.95.4.1818
45. Lyell NL, Septer AN, Dunn AK, Duckett D, Stoudenmire JL, Stabb EV. 2017. An expanded transposon mutant library reveals that *Vibrio fischeri* δ-aminolevulinate auxotrophs can colonize *Euprymna scolopes*. Appl Environ Microbiol 83:e02470-16. https://doi.org/10.1128/AEM.02470-16
46. Shaku M, Ealand C, Matlhabe O, Lala R, Kana BD. 2020. Peptidoglycan biosynthesis and remodeling revisited, p 67–103. In Gadd GM, S Sariaslani (ed), Advances in applied microbiology. Vol. 112. Academic Press.
47. Tomasz A. 1979. The mechanism of the irreversible antimicrobial effects of penicillins: how the beta-lactam antibiotics kill and lyse bacteria. Annu Rev Microbiol 33:113–137. https://doi.org/10.1146/annurev.mi.33.100179.000553
48. Cava F, Lam H, de Pedro MA, Waldor MK. 2011. Emerging knowledge of regulatory roles of D-amino acids in bacteria. Cell Mol Life Sci 68:817–831. https://doi.org/10.1007/s00018-010-0571-8
49. Kuru E, Radkov A, Meng X, Egan A, Alvarez L, Dowson A, Booher G, Breukink E, Roper DI, Cava F, Vollmer W, Brun Y, VanNieuwenhze MS. 2019. Mechanisms of incorporation for D-amino acid probes that target peptidoglycan biosynthesis. ACS Chem Biol 14:2745–2756. https://doi.org/10.1021/acschembio.9b00664
50. Walsh CT. 1989. Enzymes in the D-alanine branch of bacterial cell wall peptidoglycan assembly. J Biol Chem 264:2393–2396. https://doi.org/10.1016/S0021-9258(19)81624-1
51. Hols P, Defrenne C, Ferain T, Derzelle S, Delplace B, Delcour J. 1997. The alanine racemase gene is essential for growth of *Lactobacillus plantarum*. J Bacteriol 179:3804–3807. https://doi.org/10.1128/jb.179.11.3804-3807.1997
52. Strych U, Huang HC, Krause KL, Benedik MJ. 2000. Characterization of the alanine racemases from *Pseudomonas aeruginosa* PAO1. Curr Microbiol 41:290–294. https://doi.org/10.1007/s002840010136
53. Milligan DL, Tran SL, Strych U, Cook GM, Krause KL. 2007. The alanine racemase of *Mycobacterium smegmatis* is essential for growth in the absence of D-alanine. J Bacteriol 189:8381–8386. https://doi.org/10.1128/JB.01201-07
54. Awasthy D, Bharath S, Subbulakshmi V, Sharma U. 2012. Alanine racemase mutants of *Mycobacterium tuberculosis* require D-alanine for growth and are defective for survival in macrophages and mice. Microbiol (Reading, Engl) 158:319–327. https://doi.org/10.1099/mic.0.054064-0
55. Wei Y, Qiu W, Zhou XD, Zheng X, Zhang KK, Wang SD, Li YQ, Cheng L, Li JY, Xu X, Li MY. 2016. Alanine racemase is essential for the growth and interspecies competitiveness of *Streptococcus mutans*. Int J Oral Sci 8:231–238. https://doi.org/10.1038/ijos.2016.34
56. Wasserman SA, Walsh CT, Botstein D. 1983. Two alanine racemase genes in *Salmonella typhimurium* that differ in structure and function. J Bacteriol 153:1439–1450. https://doi.org/10.1128/jb.153.3.1439-1450.1983
57. Wild J, Hennig J, Lobocka M, Walczak W, Kłopotowski T. 1985. Identification of the dadX gene coding for the predominant isozyme of alanine racemase in *Escherichia coli* K12. Mol Gen Genet 198:315–322. https://doi.org/10.1007/BF00383013
58. Miyamoto T, Homma H. 2021. D-amino acid metabolism in bacteria. J Biochem 170:5–13. https://doi.org/10.1093/jb/mvab043
59. Richaud C, Mengin-Lecreulx D, Pochet S, Johnson EJ, Cohen GN, Marlière P. 1993. Directed evolution of biosynthetic pathways. recruitment of cysteine thioethers for constructing the cell wall of *Escherichia coli*. J Biol Chem 268:26827–26835.
60. Consaul SA, Wright LF, Mahapatra S, Crick DC, Pavelka MS. 2005. An unusual mutation results in the replacement of diaminopimelate with lanthionine in the peptidoglycan of a mutant strain of *Mycobacterium smegmatis*. J Bacteriol 187:1612–1620. https://doi.org/10.1128/JB.187.5.1612-1620.2005

61. Jones RM. Characterization of *Vibrio fischeri* mutants with altered amino acid metabolism and peptidoglycan biosynthesis. Doctor of Philosophy. University of Georgia
62. Dodds D, Bose JL, Deng M-D, Dubé GR, Grossman TH, Kaiser A, Kulkarni K, Leger R, Mootien-Boyd S, Munivar A, Oh J, Pestrak M, Rajpura K, Tikhonov AP, Turecek T, Whitfill T. 2020. Controlling the growth of the skin commensal *Staphylococcus epidermidis* using D-alanine auxotrophy. mSphere 5:e00360-20. https://doi.org/10.1128/mSphere.00360-20
63. Fuentes-Valverde V, García P, Moscoso M, Bou G. 2022. Double auxotrophy to improve the safety of a live anti-*Pseudomonas aeruginosa* vaccine. Vaccines (Basel) 10:1622. https://doi.org/10.3390/vaccines10101622
64. García P, Moscoso M, Fuentes-Valverde V, Rodicio MR, Herrera-León S, Bou G. 2023. A highly-safe live auxotrophic vaccine protecting against disease caused by non-typhoidal *Salmonella typhimurium* in mice. J Microbiol Immunol Infect 56:324–336. https://doi.org/10.1016/j.jmii.2022.10.002
65. Yang L, Lawhorn S, Bongrand C, Kosmopoulos JC, Kuwabara J, VanNieuwenhze M, Mandel MJ, McFall-Ngai M, Ruby E. 2024. Bacterial growth dynamics in a rhythmic symbiosis. Mol Biol Cell 35:ar79. https://doi.org/10.1091/mbc.E24-01-0044
66. Miller JH. 1992. A short course in bacterial genetics: A laboratory manual and handbook for *Escherichia coli* and related bacteria. Cold Spring Harbor Laboratory Press, Plainview, N.Y.
67. Stabb EV, Reich KA, Ruby EG. 2001. *Vibrio fischeri* genes hvnA and hvnB encode secreted NAD(+)-glycohydrolases. J Bacteriol 183:309–317. https://doi.org/10.1128/JB.183.1.309-317.2001
68. Visick KL, Hodge-Hanson KM, Tischler AH, Bennett AK, Mastrodomenico V. 2018. Tools for rapid genetic engineering of *Vibrio fischeri*. Appl Environ Microbiol 84:e00850-18. https://doi.org/10.1128/AEM.00850-18
69. Pollack-Berti A, Wollenberg MS, Ruby EG. 2010. Natural transformation of *Vibrio fischeri* requires tfoX and tfoY. Environ Microbiol 12:2302–2311. https://doi.org/10.1111/j.1462-2920.2010.02250.x
70. Hayashi K. 1975. A rapid determination of sodium dodecyl sulfate with methylene blue. Anal Biochem 67:503–506. https://doi.org/10.1016/0003-2697(75)90324-3
71. Gonzalez-Castro MJ, Lopez-Hernandez J, Simal-Lozano J, Oruna-Concha MJ. 1997. Determination of amino acids in green beans by derivatization with phenylisothiocianate and high-performance liquid chromatography with ultraviolet detection. J Chromatogr Sci 35:181–185. https://doi.org/10.1093/chromsci/35.4.181
72. Popham DL, Helin J, Costello CE, Setlow P. 1996. Analysis of the peptidoglycan structure of *Bacillus subtilis* endospores. J Bacteriol 178:6451–6458. https://doi.org/10.1128/jb.178.22.6451-6458.1996